Journal of Applied Sciences

ISSN 1812-5654

science alert

ANSInet
an open access publisher
http://ansinet.com

Journal of Applied Sciences 8 (22): 4029-4039, 2008
ISSN 1812-5654

The Effect of Vertical Component of Earthquake on Seismic Response of Torsionally Coupled Systems

[1,2]M.F. Nezamabadi, [3]A.S. Moghadam and [3]M. Hosseini
[1]Structure and Earthquake Group in Science and Research Branch, The Islamic Azad University, Iran
[2]Department of Civil Engineering, The Islamic Azad University, South Tehran Branch,
P.O. Box 14515-775, 14155-4933, Tehran, Iran
[3]Structural Engineering Research Center,
The International Institute of Earthquake Engineering and Seismology, P.O. Box 19395-3913, Tehran, Iran

Abstract: A compendium of field observations in recent years in near field as Northridge (1994), Kobe (1995), Turkish (1995), Athens (1999), Bam (2003) and past analytical investigations have shown that the vertical component have significant effect in creating seismic damage. Also assessment of structural performances during past earthquakes demonstrates that plan irregularity, due to asymmetric distribution of mass, stiffness and strength, is one of the most frequent sources of severe damage. In this study the effects of vertical component of earthquake motion, acting simultaneously with horizontal component on the structures with asymmetric distribution of mass have been studied. A simple lumped-mass model of a single storey building resting on a rigid foundation with 4 degrees of freedom; the lateral displacement, the torsional displacement, the vertical displacement and the rotational displacement about lateral axis has been developed and displacement responses have been evaluated subjected to horizontal, torsional, vertical and rotational motions. The mass of diaphragm has been assumed to act at an eccentricity (e) from the center of resistance about x-axis and z-axis. It has been concluded that the influence of higher values of eccentricity ratio is to increase horizontal and vertical responses for smaller frequency ratio values. Increasing rate of vertical response due to eccentricity is reduced with decreasing frequency ratio values. Vertical response is very sensitive to the vertical frequency ratio values. For smaller vertical frequency ratio values, the response is much higher when the translational natural period of uncoupled building is greater than 1.2 sec.

Key words: Seismic response, asymmetric distribution of mass, frequency ratio value, eccentricity ratio value

INTRODUCTION

A compendium of field observations and analytical results indicate that certain failure modes are more convincingly attributable to high vertical earthquake-induced forces. In addition to the possibility of compressive overstressing or failure due to direct tension, vertical motion may induce failure in shear and flexure. Under reduced compression or mild tension, the contribution of concrete to shear resistance is eroded, thus many observed shear failure modes may have underlying vertical motion effects (Papazoglou and Elnashai, 1996).

The presence of the vertical excitation can produce a variation in the distribution of the dissipated energy among the elements of the frames, with a possible greater demand in the columns (Decaninni *et al*., 2002).

The main effect of the vertical motion consists of the variation of axial force in the columns. The high values of compression, or even tension, induced by the vertical excitation could produce damage in the structure which leads to a decrease of structural capacity to withstand the horizontal seismic motion, resulting in an increase of horizontal displacements (Papazoglou and Elnashai, 1996; Decaninni *et al*., 2002; Diotallevi and Landi, 2000; Kikuchi and Yoshimura, 1984; Hosseini and Nezamabadi, 2004; Wang *et al*., 1989).

The varying axial force in the columns results in pinched hysteretic behavior that causes larger horizontal displacement and column end moments and curvature (Diotallevi and Landi, 2006; Foutch, 1997).

The vertical component has the important effect of changing the plastic hinge distribution, sequence of hinging and mode of failure of the structure (Diotallevi and Landi, 2006; Ghobarah and Elnashai, 1998). Vertical ground acceleration in near-source regions can increase the design forces for connections of heavy nonstructural cladding panels (Memari *et al*., 2004).

Corresponding Author: Maryam Firoozi Nezamabadi, No. 31, Niloofar 13 Block, Sharak e Shahid Beheshti, Babaei Highway, Tehran, Zip Code 16511-14766, Iran Tel: +98-21-7711-5627 Fax: +98-21-7711-6476

The responses subjected to vertical acceleration (V) are usually taken into consideration by using about two thirds of the horizontal response spectra (H). However, recent studies have shown that the V/H response spectral ratio depends on the distance of the site to the seismic source. The ratio is higher in the near-field region and in the high-frequency range of the response spectra. The V/H ratio largely exceeds the commonly assumed ratio of two thirds at short periods in the near-field regions. As a result, the margin of safety of structures subjected to an earthquake in the near-field regions is questionable (Kianoush and Chen, 2006; Xinle *et al*., 2007).

Assessment of structural performances during past earthquakes demonstrates that plan irregularity, due to asymmetric distribution of mass, stiffness and strength, is one of the most frequent sources of severe damage, since it results in floor rotations (torsional response) in addition to floor translations. In past years, large research efforts have been devoted to the study of the seismic response of asymmetric structures, both in the elastic and inelastic range of behavior (Rutenberg, 1998). In particular, inelastic behavior is of great interest since the ability of structures to resist strong earthquakes depends upon their ductility and capacity for energy dissipation.

Most of these studies were conducted by using simple single storey asymmetric models. Simplified models neglect important effects that may influence inelastic behavior of resisting elements and in turn, of the entire structure. Namely, resisting elements are assumed to resist uni-directional horizontal forces only; therefore, no allowance for interaction among bi-directional horizontal and vertical forces in resisting elements is usually made (Stefano and Pintucchi, 2002).

One of the past investigations that have considered the effect of vertical component of earthquake motion acting simultaneously with horizontal component on the torsionally coupled structures has been done by Gupta and Hutchinson (1994). They have evaluated the displacement response of a simple lumped mass model of a single story building resting on a rigid foundation with three degree of freedom: firstly, the lateral displacement (u), secondly, the torsional displacement, u_θ and thirdly, the vertical displacement, w. The mass of diaphragm was acting at an eccentricity (e) from the center of resistance (Fig. 1a, b). The mass of vertical elements (columns) of building was lumped in line with the center of resistance and the mass of the diaphragm in z direction was ignored to avoid creating eccentricity in the vertical direction.

In this study, the model has been improved by adding one degree of freedom, rotation about x-axis and considering eccentricity (e) of vertical masses.

In response analysis, it has been assumed that the earthquake ground motion input in horizontal and vertical direction $\ddot{u}_{g(t)}$ and $\ddot{v}_g(t)$, are applied uniformly over the base of structure. The displacement responses subjected to horizontal motion (u), the torsional motion (u_θ), the combined horizontal and torsional ($u+u_\theta$), the vertical motion (v), the rotational motion about x axes (v_θ) and finally the combined vertical and rotational ($v+v_\theta$) have been evaluated in terms of time history displacement for the El-Centro earthquake, N-S, 1940.

STRUCTURAL SYSTEM

A single story building, shown in Fig. 1a, c consists of a rigid floor diaphragm of radius r supported on elastic column has been considered. The four degrees of freedom of the system are: the lateral displacement (u) of the floor relative to the ground along the principal axis of resistance (x) of the building; the torsional displacement (u_θ) of the floor about the vertical axis (z); the vertical displacement (v) of supporting columns, relative to the ground along the principal axis of resistance (z) of the building and rotational displacement (v_θ) of the floor about the horizontal axis (x).

The total mass of the floor is represented by m. The structural eccentricity (e), between the center of mass and resistance is caused by different mass densities ($\rho_a, \rho_b; \rho_a > \rho_b$) in the two halves of the equivalent floor disc, split along y = 0, as shown in Fig. 1a. The principal axis of resistance coincide with the x and y horizontal axis of the reference system. The principal axis of resistance in the vertical direction coincides with the z axis of the reference system. Rotational displacements (θ) of the disc about z and x-axis take place about the center of resistance (x = y = 0).

The response displacements of the floor diaphragm have been assumed to be sufficiently small to ensure the structural stability and therefore, the effects of changes in the geometry may be neglected. The damping ratio (ζ) is taken as 5% of critical damping.

EQUATION OF MOTION

The Equations of motion of the building model (Fig. 1a, c) are derived from the dynamic equilibrium for each degree of freedom.

x-direction:

$$m\ddot{u} + me\ddot{\theta}_z + C_{uu}\dot{u} + C_{u\theta}\dot{\theta} + k_u u = -m\ddot{u}_g \quad (1)$$

Rotation about z direction (θ_z):

$$I_{oz}\ddot{\theta}_z + me\ddot{u} + C_{\theta\theta z}\dot{\theta}_z + C_{u\theta}\dot{u} + k_{\theta z}\theta_z = -me\ddot{u}_g \quad (2)$$

z-direction:

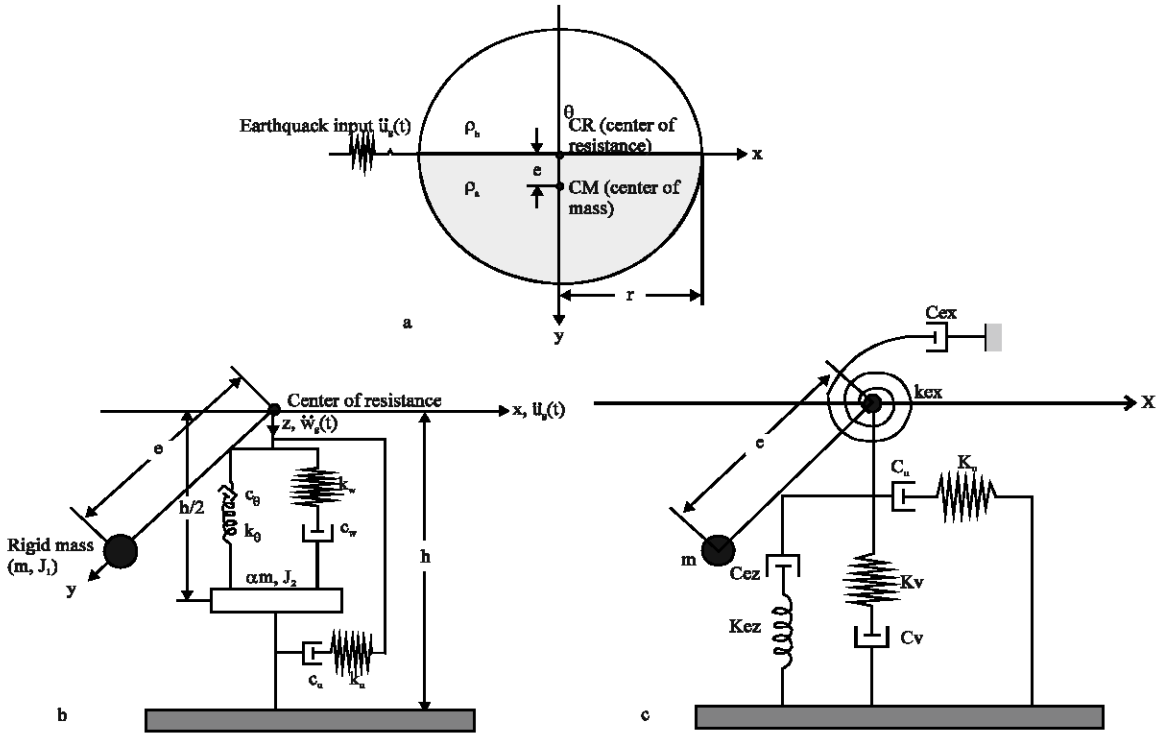

Fig. 1: Lumped mass model of a single storey building; (a, b) the model developed by Gupta and Hutchinson (1994) and (a, c) the model improved in this study

$$m\ddot{v} + me\ddot{\theta}_x + C_{vv}\dot{v} + C_{v\theta}\dot{\theta} + k_v v = -m\ddot{v}_g \tag{3}$$

Rotation about x direction (θ_x):

$$I_{\alpha x}\ddot{\theta}_x + me\ddot{v} + C_{\theta\theta x}\dot{\theta}_x + C_{v\theta}\dot{v} + k_{\theta x}\theta_x = -me\ddot{v}_g \tag{4}$$

Substituting;

$$u_\theta = r \times \theta_z, v_\theta = r \times \theta_x, e_r = e/r, I_{\alpha x} = \frac{mr^2}{2}, I_{\alpha x} = \frac{mr^2}{4}$$

and writing Eq. 1-4 in matrix form we obtain:

$$[M]\{\ddot{u}\} + [C]\{\dot{u}\} + [K]\{u\} = -\{\ddot{u}_g\} \tag{5a}$$

$$\begin{bmatrix} 1 & e_r & 0 & 0 \\ e_r & 1/2 & 0 & 0 \\ 0 & 0 & 1 & e_r \\ 0 & 0 & e_r & 1/4 \end{bmatrix} \begin{Bmatrix} \ddot{u} \\ \ddot{u}_\theta \\ \ddot{v} \\ \ddot{v}_\theta \end{Bmatrix} + \begin{bmatrix} C_{uu}/m & C_{u\theta}/mr & 0 & 0 \\ C_{u\theta}/mr & C_{\theta\theta z}/mr^2 & 0 & 0 \\ 0 & 0 & C_{vv}/m & C_{v\theta}/mr \\ 0 & 0 & C_{v\theta}/mr & C_{\theta\theta x}/mr^2 \end{bmatrix} \begin{Bmatrix} \dot{u} \\ \dot{u}_\theta \\ \dot{v} \\ \dot{v}_\theta \end{Bmatrix}$$

$$+ \begin{bmatrix} k_u/m & 0 & 0 & 0 \\ 0 & k_{\theta z}/mr^2 & 0 & 0 \\ 0 & 0 & k_v/m & 0 \\ 0 & 0 & 0 & k_{\theta x}/mr^2 \end{bmatrix} \begin{Bmatrix} u \\ u_\theta \\ v \\ v_\theta \end{Bmatrix} = -\begin{Bmatrix} \ddot{u}_g \\ e_r\ddot{u}_g \\ \ddot{v}_g \\ e_r\ddot{v}_g \end{Bmatrix} \tag{5b}$$

where, [M],[C],[K] and $\{\ddot{u}_g\}$ are mass, damping, stiffness and ground motion matrices, respectively.

Evaluation of damping matrix coefficients

Considering classical damping:

$$C = a[M] + b[K] \tag{6}$$

where, a and b are arbitrary proportionality factors and are determined by assuming that both the natural modes of vibration (u and u_θ) of the coupled system have the same ratio ζ of critical damping. The damping matrix proportional to the mass and/or stiffness matrices will permit uncoupling the Equation of motion. For each mode the generalized damping is given by:

$$C_i = \varphi_i^T C \varphi_i = 2\xi_i \omega_i M_i \tag{7}$$

$$C_i = \varphi_i^T C \varphi_j = 0 \qquad i \neq j \tag{8}$$

where, ω_i is the natural frequency of the coupled system in mode i and ζ is the modal damping ratio.

$$\varphi_i^T (aM + bK)\varphi_i = 2\xi_i \omega_i M_i \tag{9}$$

$$aM_i + bK_i = 2\xi_i\omega_i M_i \quad (\omega_i^2 = \frac{K_i}{M_i}) \tag{10}$$

$$a + b\omega_i^2 = 2\xi_i\omega_i;\ \ i = 1,2 \tag{11}$$

Solving above Equations yields:

$$a = \frac{2\xi\omega_1\omega_2}{\omega_1 + \omega_2} \qquad b = \frac{2\xi}{\omega_1 + \omega_2} \tag{12}$$

where, ω_1 and ω_2 are the fundamental and secondary natural frequencies of the coupled system.
Substituting a and b into Eq. 6 yields:

$$[C] = \frac{2\xi\omega_1\omega_2}{\omega_1 + \omega_2}\begin{bmatrix} 1 & e_r & 0 & 0 \\ e_r & 1/2 & 0 & 0 \\ 0 & 0 & 1 & e_r \\ 0 & 0 & e_r & 1/4 \end{bmatrix} + \frac{2\xi}{\omega_1 + \omega_2}\begin{bmatrix} k_u/m & 0 & 0 & 0 \\ 0 & k_{\theta z}/mr^2 & 0 & 0 \\ 0 & 0 & k_v/m & 0 \\ 0 & 0 & 0 & k_{\theta x}/mr^2 \end{bmatrix} \tag{13}$$

Comparing Eq. 13 and 5:

$$\frac{C_{uu}}{m} = \frac{2\xi\omega_1\omega_2}{\omega_1 + \omega_2} + \frac{2\xi}{\omega_1 + \omega_2}(\frac{K_u}{m}) \tag{14}$$

$$\frac{C_{\theta\theta z}}{mr^2} = \frac{\xi\omega_1\omega_2}{\omega_1 + \omega_2} + \frac{2\xi}{\omega_1 + \omega_2}(\frac{K_{\theta z}}{mr^2}) \tag{15}$$

$$\frac{C_{vv}}{m} = \frac{2\xi\omega_1\omega_2}{\omega_1 + \omega_2} + \frac{2\xi}{\omega_1 + \omega_2}(\frac{K_v}{m}) \tag{16}$$

$$\frac{C_{\theta\theta x}}{mr^2} = \frac{\xi\omega_1\omega_2}{2(\omega_1 + \omega_2)} + \frac{2\xi}{\omega_1 + \omega_2}(\frac{K_{\theta x}}{mr^2}) \tag{17}$$

$$\frac{C_{u\theta}}{mr} = \frac{C_{v\theta}}{mr} = \frac{2\xi\omega_1\omega_2}{\omega_1 + \omega_2}e_r \tag{18}$$

where, ω_u, $\omega_{\theta z}$, ω_v, $\omega_{\theta x}$ represent the translational, torsional, vertical and rotational natural frequencies, respectively, of the corresponding torsionally uncoupled building (zero eccentricity):

$$k_u = m\omega_u^2 \tag{19}$$

$$k_{\theta z} = I_{oz}\omega_{\theta z}^2 = \frac{mr^2}{2}\omega_{\theta z}^2 \tag{20}$$

$$k_v = m\omega_v^2 \tag{21}$$

$$k_{\theta x} = I_{ox}\omega_{\theta x}^2 = \frac{mr^2}{4}\omega_{\theta x}^2 \tag{22}$$

By defining:

$$\lambda_{Tz} = \frac{\omega_{\theta z}}{\omega_u}$$

$$\lambda_v = \frac{\omega_v}{\omega_u}$$

$$\lambda_{Tx} = \frac{\omega_{\theta x}}{\omega_u}$$

$$\Omega_n = \frac{\omega_n}{\omega_u}$$

from Eq. 14-18 damping matrix coefficients are obtained as function of frequency ratio value.

$$C_{uu} = \frac{2\xi\omega_1\omega_2 m}{\omega_1 + \omega_2} + \frac{2\xi m\omega_u^2}{(\omega_1 + \omega_2)} = 2\xi m\omega_1\left[\frac{1}{\Omega_1 + \Omega_2}\right]\left[\Omega_2 + \frac{1}{\Omega_1}\right] = 2\xi m\omega_1 D_{uu} \tag{23}$$

$$C_{\theta\theta z} = \frac{\xi\omega_1\omega_2}{\omega_1 + \omega_2}mr^2 + \frac{2\xi K_{\theta z}}{\omega_1 + \omega_2} = \xi\omega_1 mr^2\left[\frac{1}{\Omega_1 + \Omega_2}\right]\left[\Omega_2 + \frac{\lambda_{Tz}^2}{\Omega_1}\right] = \xi\omega_1 mr^2 D_{\theta\theta z} \tag{24}$$

$$C_{vv} = \frac{2\xi m\omega_1\omega_2}{\omega_1 + \omega_2} + \frac{2\xi m\omega_v^2}{(\omega_1 + \omega_2)} = 2\xi m\omega_1\left[\frac{\Omega_2}{\Omega_1 + \Omega_2}\right]\left[1 + \frac{\lambda_v^2}{\Omega_1\Omega_2}\right] = 2\xi m\omega_1 D_{vv} \tag{25}$$

$$C_{\theta\theta x} = \frac{\xi\omega_1\omega_2(mr^2)}{2(\omega_1 + \omega_2)} + \frac{2\xi}{\omega_1 + \omega_2}K_{\theta x} = \frac{1}{2}mr^2\xi\omega_1\left[\frac{1}{\Omega_1 + \Omega_2}\right]\left[\Omega_2 + \frac{\lambda_{Tx}^2}{\Omega_1}\right] = \frac{1}{2}mr^2\xi\omega_1 D_{\theta\theta x} \tag{26}$$

$$C_{u\theta} = C_{v\theta} = \frac{2\xi\omega_1\omega_2}{\omega_1 + \omega_2} \times mr \times \frac{e}{r} = 2\xi\omega_1 me\left[\frac{\Omega_2}{\Omega_1 + \Omega_2}\right] = 2\xi\omega_1 me D_{u\theta} \tag{27}$$

By substituting damping matrix coefficient (Eq. 23-27) into damping matrix, it is obtained:

$$C = 2\xi m\omega_1\begin{bmatrix} D_{uu} & eD_{u\theta} & 0 & 0 \\ eD_{u\theta} & \frac{1}{2}r^2D_{\theta\theta z} & 0 & 0 \\ 0 & 0 & D_{vv} & eD_{v\theta} \\ 0 & 0 & eD_{v\theta} & \frac{1}{4}r^2D_{\theta\theta x} \end{bmatrix} \tag{28}$$

NATURAL FREQUENCIES

The undamped natural frequencies of the system are determined from a free vibration analysis as the following:

$$\begin{bmatrix} 1 & e_r & 0 & 0 \\ e_r & \frac{1}{2} & 0 & 0 \\ 0 & 0 & 1 & e_r \\ 0 & 0 & e_r & \frac{1}{4} \end{bmatrix}\begin{Bmatrix} \ddot{u} \\ \ddot{u}_\theta \\ \ddot{v} \\ \ddot{v}_\theta \end{Bmatrix} + \begin{bmatrix} \frac{k_u}{m} & 0 & 0 & 0 \\ 0 & \frac{k_{\theta z}}{mr^2} & 0 & 0 \\ 0 & 0 & \frac{k_v}{m} & 0 \\ 0 & 0 & 0 & \frac{k_{\theta x}}{mr^2} \end{bmatrix}\begin{Bmatrix} u \\ u_\theta \\ v \\ v_\theta \end{Bmatrix} = \begin{Bmatrix} 0 \\ 0 \\ 0 \\ 0 \end{Bmatrix} \tag{29}$$

Since:

$$\frac{k_u}{m} = \omega_u^2 = \frac{\omega_1^2}{\Omega_1^2} \quad (30)$$

$$\frac{k_{\theta z}}{mr^2} = \frac{1}{2}\omega_{\theta z}^2 = \frac{1}{2}\lambda_{Tz}^2\omega_u^2 = \frac{1}{2}\lambda_{Tz}^2\frac{\omega_1^2}{\Omega_1^2} \quad (31)$$

$$\frac{k_v}{m} = \omega_v^2 = \lambda_v^2\omega_u^2 = \lambda_v^2\frac{\omega_1^2}{\Omega_1^2} \quad (32)$$

$$\frac{k_{\theta x}}{mr^2} = \frac{1}{4}\omega_{\theta x}^2 = \frac{1}{4}\lambda_{Tx}^2\omega_u^2 = \frac{1}{4}\lambda_{Tx}^2\frac{\omega_1^2}{\Omega_1^2} \quad (33)$$

Equation 29 becomes:

$$\begin{bmatrix} 1 & e_r & 0 & 0 \\ e_r & \frac{1}{2} & 0 & 0 \\ 0 & 0 & 1 & e_r \\ 0 & 0 & e_r & \frac{1}{4} \end{bmatrix} \begin{Bmatrix} \ddot{u} \\ \ddot{u}_\theta \\ \ddot{v} \\ \ddot{v}_\theta \end{Bmatrix} + \frac{\omega_1^2}{\Omega_1^2} \begin{bmatrix} 1 & 0 & 0 & 0 \\ 0 & \frac{1}{2}\lambda_{Tz}^2 & 0 & 0 \\ 0 & 0 & \lambda_v^2 & 0 \\ 0 & 0 & 0 & \frac{1}{4}\lambda_{Tx}^2 \end{bmatrix} \begin{Bmatrix} u \\ u_\theta \\ v \\ v_\theta \end{Bmatrix} = \begin{Bmatrix} 0 \\ 0 \\ 0 \\ 0 \end{Bmatrix} \quad (34)$$

The frequency determinant may be written by simplifying.

$$\begin{vmatrix} (\frac{\omega_1^2}{\Omega_1^2} - \omega^2) & -e_r\omega^2 & 0 & 0 \\ -e_r\omega^2 & \frac{1}{2}(\frac{\omega_1^2}{\Omega_1^2}\lambda_{Tz}^2 - \omega^2) & 0 & 0 \\ 0 & 0 & (\frac{\omega_1^2}{\Omega_1^2}\lambda_v^2 - \omega^2) & -e_r\omega^2 \\ 0 & 0 & -e_r\omega^2 & \frac{1}{4}(\frac{\omega_1^2}{\Omega_1^2}\lambda_{Tx}^2 - \omega^2) \end{vmatrix} = 0 \quad (35)$$

TIME HISTORY ANALYSIS

For comparing the results of this study with those of the study developed by Gupta and Hutchinson (1994), El-Centro record has been used in time history analysis. For the purpose of computing the vertical displacement response subjected to El-Centro earthquake, 100% of the N-S has been assumed to be acting in the vertical direction. The peak displacement of this record is 20.91 cm, the peak velocity is 32.48 cm sec^{-1} and the peak acceleration is 0.312 g.

Three structural models have been prepared and analyzed: first, the new model, presented in this study, second, the model presented by Gupta and Hutchinson (1994), third the model presented by Gupta and Hutchinson (1994) in which there are 6 degrees of freedom and distributed vertical springs in perimeter of slab. These three models have been analyzed for three values of frequency ratios ($\lambda = \lambda_{Tx} = \lambda_v = \lambda_{Tz} = 0.6$, 1.0 and 1.4) and two values of eccentricity ratios (e_r = 0.15 and 0.30) separately. In order to develop displacement response spectra, for each eccentricity ratio value and each frequency ratio value, analysis have been repeated for ten values of uncoupled natural period (T_u = 0.2, 0.4, 0.6, 0.8, 1.0, 1.2, 1.4, 1.6, 1.8, 2.0). At first, first and second models have been analyzed by using MATLAB software and then three models have been analyzed by using SAP2000. In analysis it has been assumed that the earth ground acceleration input in horizontal and vertical direction is applied uniformly over the base of the structure. The structure have been modeled to be resting on a rigid foundation, hence interaction effects have been neglected.

TIME HISTORY ANALYSIS RESULTS

In the present study the individual response quantities have been computed separately as a complete time history; the response maxima u_{max}, $u_{\theta max}$, v_{max} and $v_{\theta max}$ have been then selected as appropriate. These maximum displacement responses are presented in normalized form in Fig. 2-7. In each figure, response curves have been normalized to the maximum quantity in the earthquake ground motion records and plotted as a function of the uncoupled natural period (T_u). As it is expected the horizontal displacement response curves of center of resistance and edges are quite close to each other for all frequency ratio values and all eccentricity ratio values. For example, horizontal displacement response curves of center of resistance and edges for λ_{Tz} = 1.0 and e_r = 0.30 are shown in Fig. 2.

The vertical displacements of edges in each time step are obtained as ($v+v_\theta$) and ($v-v_\theta$) where v is the vertical displacement of center of resistance and v_θ is rotational displacement about x-axis. The normalized vertical displacement curves are shown in Fig. 3-5. Paying attention to these figures, one can observe that:

Large frequency ratio value (λ = 1.4)

- The vertical displacement curves of center of resistance are quite close to each other for e_r = 0.15 in entire range of T_u = 0 to 1.0 sec
- The vertical response curve of center of resistance of second model is upper than the other models for e_r = 0.30 while the vertical response curve of edges of this model is lower than the others because of rotation resulting from mass eccentricity
- The edges displacement response of second and third models are close to each other for e_r = 0.15 while the response curve corresponding to first model exceeds the other two response curves for e_r = 0.30

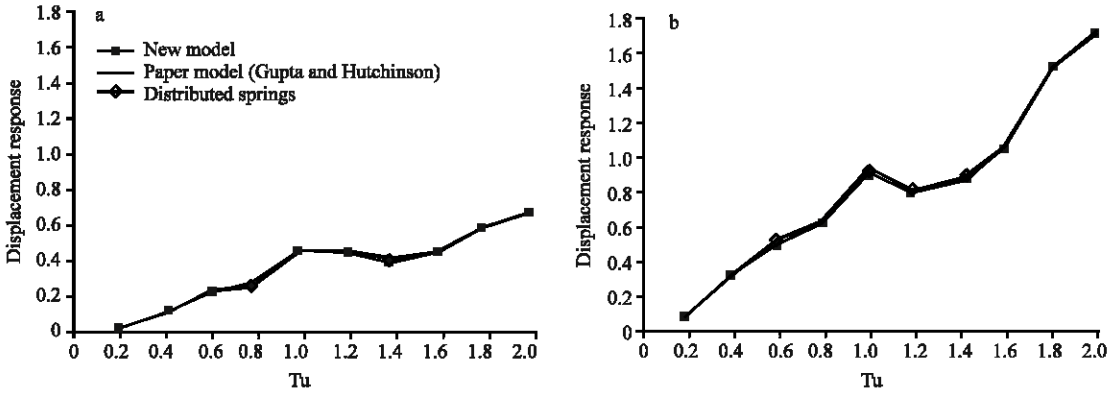

Fig. 2: Normalized horizontal displacement response spectra (λ_{Tz} = 1.0, e_r = 0.30); (a) translational displacement of center of resistance and (b) maximum translational displacement

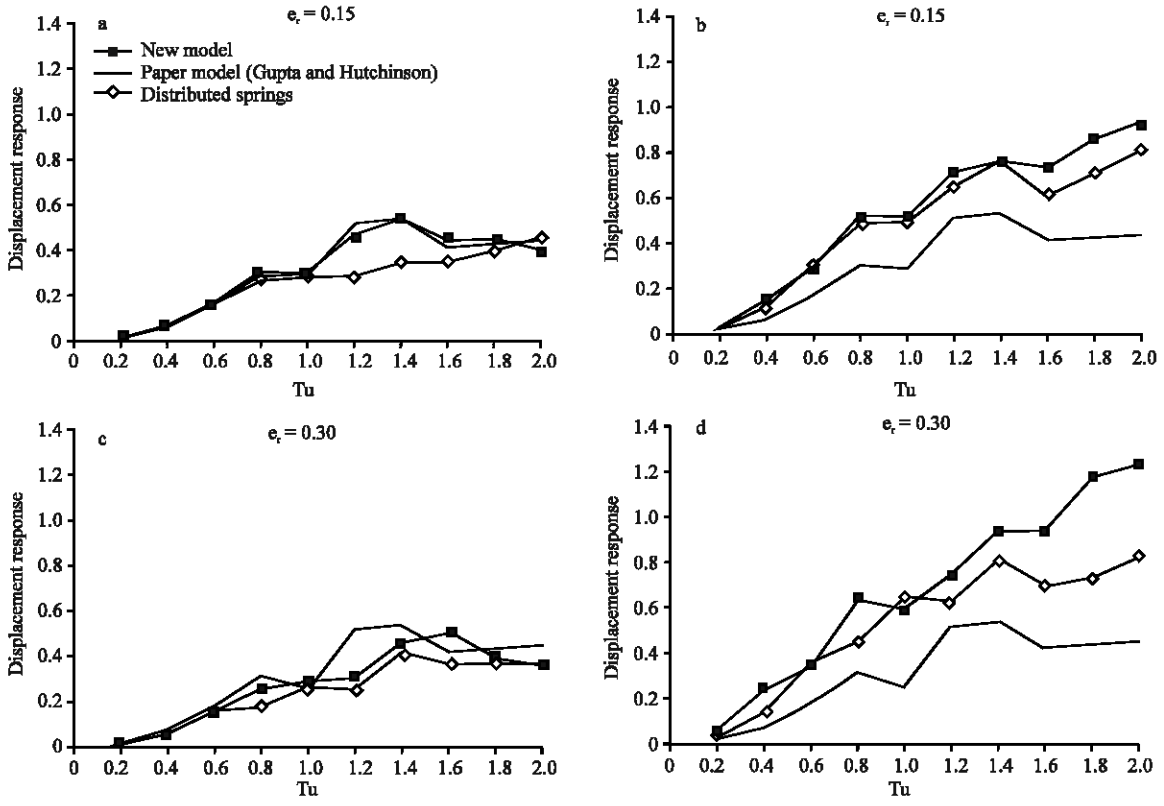

Fig. 3: Normalized vertical displacement response spectra (λ_{Tz} = λ_{Tx} = λ_v = 1.4); (a, c) vertical displacement of center of resistance and (b, d) maximum vertical displacement of edges

- The edges responses increase up to 24% when eccentricity ratio value is increased (Fig. 3)

Intermediate frequency ratio value (λ = 1.0)

- The vertical displacement curves of center of resistance are close to each other for e_r = 0.15 when uncoupled natural period is less than 0.8 sec and more than 1.2 sec
- The edges displacement response trends of first and third models are about the same for e_r = 0.15 while the response curve corresponding to first model exceeds the other two response curves for e_r = 0.30

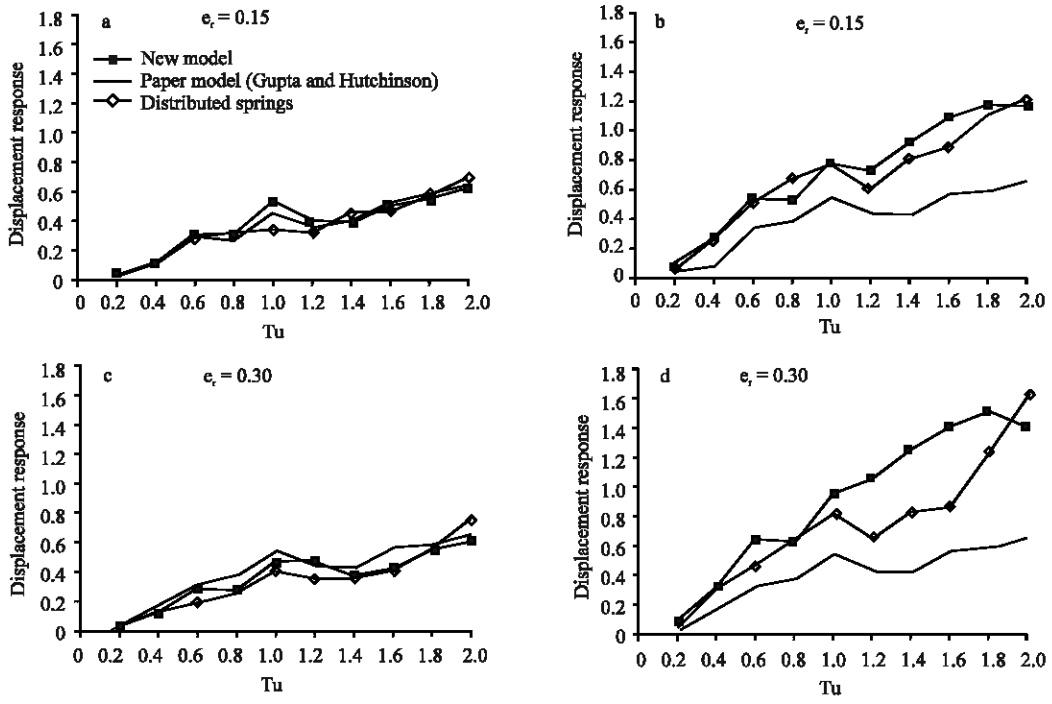

Fig. 4: Normalized vertical displacement response spectra ($\lambda_{Tz} = \lambda_{Tx} = \lambda_v = 1.0$); (a, c) vertical displacement of center of resistance and (b, d) maximum vertical displacement of edges

- The edges responses increase up to 21% when eccentricity ratio value is increased (Fig. 4)

Small frequency ratio value ($\lambda = 0.6$)

- The vertical displacement curves of center of resistance are close to each other for $e_r = 0.15$ in entire range of $T_u = 0$ to 1.2 sec and for $e_r = 0.30$ when uncoupled natural period is less than 1.0 sec
- The edges displacement response trends of first and third models are about the same for $e_r = 0.15$ while the response curve corresponding to first model exceeds the other two response curves for $e_r = 0.30$ when uncoupled natural period is less than 1.0 sec
- The edges responses increase up to 14% when eccentricity ratio value is increased (Fig. 5)

By comparing the results of various frequency ratio values it is found that the response differences decrease with decreasing frequency ratio values (λ) for all eccentricity ratio values. In fact the increasing rate of vertical response due to eccentricity is reduced by decreasing torsional and rotational rigidity.

Normalized translational displacement curves corresponding of first model are shown in Fig. 6 for various frequency ratio values. The response curves are close together when uncoupled natural period is less than 0.8 sec and then the curves corresponding to $\lambda = 0.6$ exceeds the other two response curves up to $T_u = 1.6$ sec.

The higher response is obtained for the curve $\lambda = 1.0$ when $T_u \geq 1.6$ sec. The maximum translational displacement of edges is about 0.6 for all frequency ratio values and for all eccentricity ratio values when $T_u = 0.8$ sec.

Normalized vertical displacement curves corresponding of first model are shown in Fig. 7 for various frequency ratio values. The response curve corresponding to $\lambda = 0.6$ exceeds the other two response curves for $\lambda = 1.0$ and $\lambda = 1.4$ over the entire range of uncoupled natural period values. There is a sharp increase when $T_u \geq 1.2$ sec. This result is similar to result presented in the study of Gupta and Hutchinson (1994).

The response values are the same when $T_u = 0.8$ sec. for $\lambda = 1.0$ and $\lambda = 1.4$. When $T_u = 1.0$ sec the response values are the same for $\lambda = 0.6$ and $\lambda = 1.0$ except for the maximum vertical displacement response for $e_r = 0.30$. The vertical displacement response increases significantly when the eccentricity ratio value is increased.

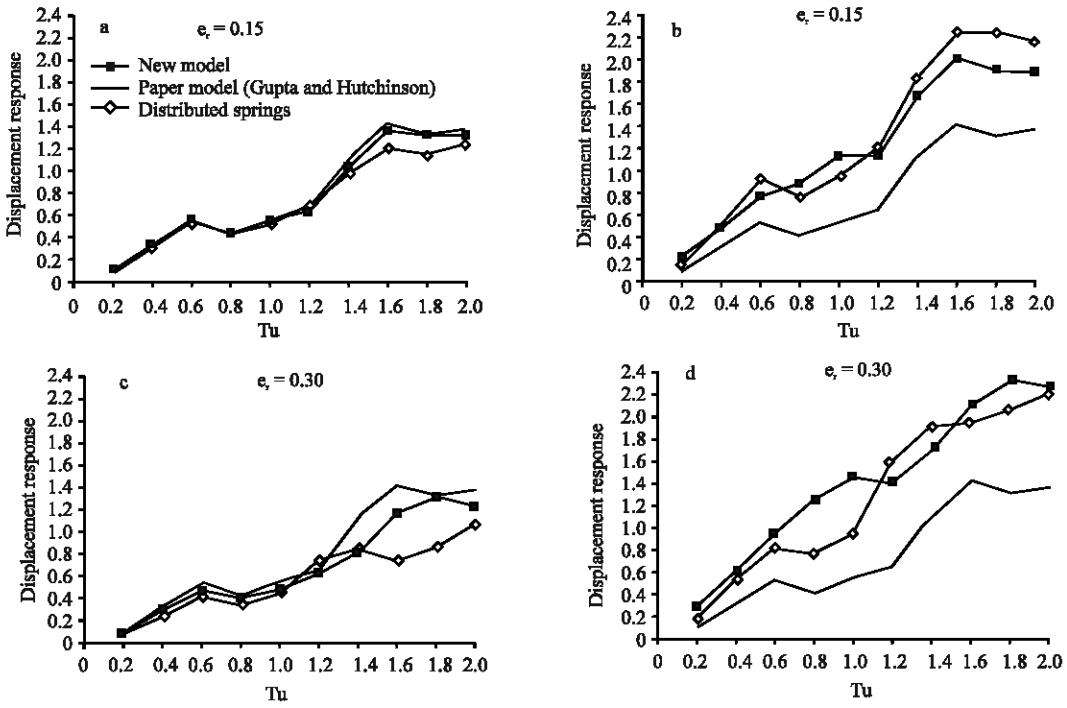

Fig. 5: Normalized vertical displacement response spectra ($\lambda_{Tz} = \lambda_{Tx} = \lambda_v = 0.6$); (a, c) vertical displacement of center of resistance and (b, d) maximum vertical displacement of edges

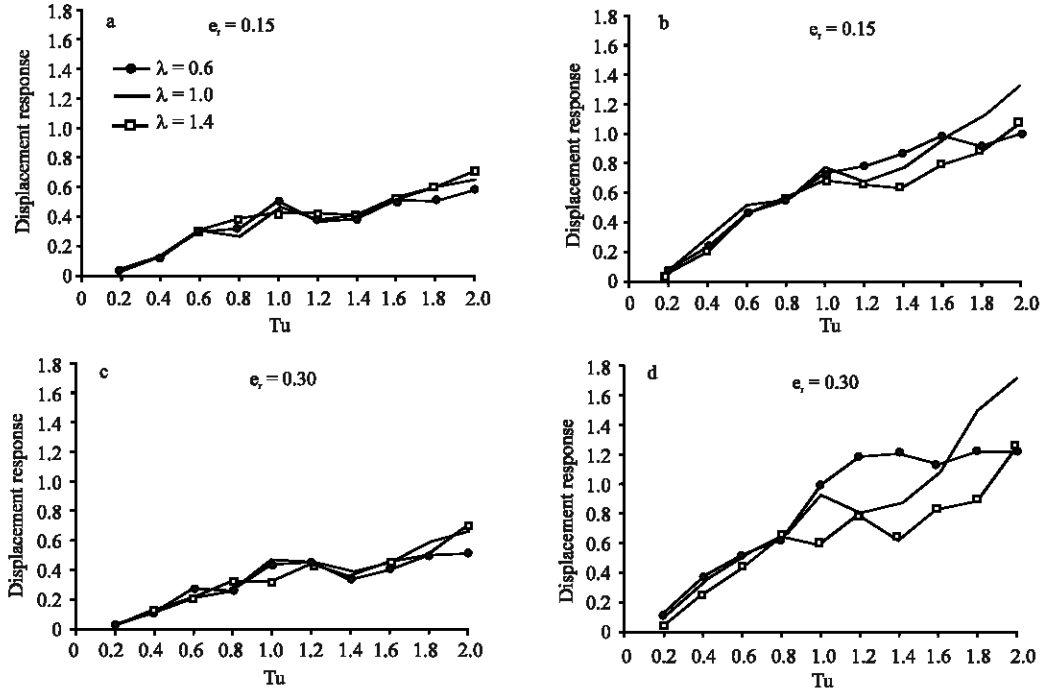

Fig. 6: Normalized translational displacement response spectra for new model; (a, c) translational displacement of center of resistance and (b, d) maximum translational displacement

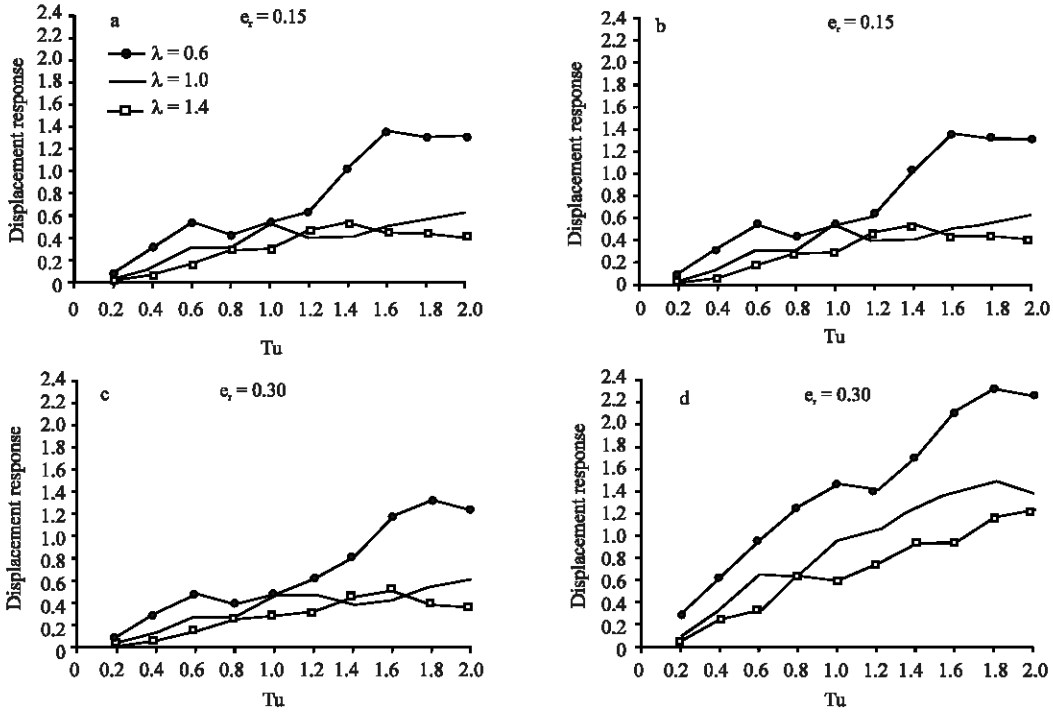

Fig. 7: Normalized vertical displacement response spectra for new model; (a, c) vertical displacement of center of resistance and (b, d) maximum vertical displacement of edges

CONCLUSION

In this study, a simple lumped-mass model of a single story building resting on a rigid foundation with four degrees of freedom has been developed. The mass of diaphragm (m) has been assumed to act at an eccentricity (e) from the center of resistance (first model). Second model is model presented by Gupta and Hutchinson (1994) and third model is the model of Gupta and Hutchinson (1994) with 6 degrees of freedom and distributed vertical springs in perimeter of slab.

Results of first model have been compared with results of the other two models. Analysis have been carried out for three values of frequency ratio and for two values of eccentricity. In order to develop displacement response spectra, for each eccentricity ratio value and each frequency ratio value, analysis have been repeated for ten values of uncoupled natural period. The following results can be obtained:

- The horizontal displacement response curves of center of resistance and edges are quite close to each other for all frequency ratio values and all eccentricity ratio values
- The vertical displacement response of center of resistance are close together when uncoupled natural period is smaller than 1.0 sec, while the vertical displacement responses of edges corresponding to proposed model exceeds the other two model in this interval
- The influence of higher eccentricity ratio value (e_r) is to increase the translational and vertical responses for smaller frequency ratio values (λ)
- The torsional and rotational responses increase significantly when the eccentricity ratio value (e_r) is increased
- The vertical response is very sensitive to the frequency ratio values (λ). For smaller frequency ratio values, the response is much higher when uncoupled natural period is greater than 1.2 sec
- Increasing rate of vertical response due to eccentricity ratio value is reduced with decreasing frequency ratio values (λ). In fact reduction of tortional and rotational rigidity in comparison with translational rigidity results in reduction of response differences
- The responses obtained from proposed model are more than those of the other two models in most cases and are increased when frequency ratio values (λ) decrease

Base of the above results it can be concluded that the proposed model leads to more conservative response value in the period range of zero to one second which is the period range of short to mid story building.

Further studies are required for the case of eccentricities in 2 direction of x and y.

Notation:

a, b	=	Rayleigh's damping constants
C_{uu}, $C_{u\theta}$, $C_{\theta\theta z}$, C_{vv}, $C_{v\theta}$, $C_{\theta\theta x}$	=	Coefficients of damping matrix
C	=	Damping matrix
C_i	=	Generalized damping in mode i
D_{uu}, $D_{u\theta}$, $D_{\theta\theta z}$, D_{vv}, $D_{v\theta}$, $D_{\theta\theta x}$	=	Dimensionless damping coefficient
e	=	Structural eccentricity
e_r	=	Eccentricity ratio value (e/r)
g	=	Gravity acceleration
k_u, $k_{\theta z}$, k_v, $k_{\theta x}$	=	Lateral, tortional, vertical and rotational story stiffness, respectively
M	=	Mass matrix
K	=	Stiffness matrix
r	=	Radius of equivalent floor disk
t	=	Time
T_u	=	Uncoupled natural period
u, u_θ, v, v_θ	=	Time history of translational, torsional, vertical and rotational displacement of floor, respectively
$u, \dot{u}, \ddot{u}$	=	Time history of displacement, velocity and acceleration in lateral direction of building
$u_\theta, \dot{u}_\theta, \ddot{u}_\theta$	=	Time history of torsional displacement, torsional velocity and torsional acceleration of building
$v, \dot{v}, \ddot{v}$	=	Time history of displacement, velocity and acceleration in vertical direction of building
$v_\theta, \dot{v}_\theta, \ddot{v}_\theta$	=	Time history of rotational displacement, rotational velocity and rotational acceleration of building
x, y, z	=	Cartesian axes of reference
ζ	=	Viscous damping ratio
$\lambda_{Tz}, \lambda_v, \lambda_{Tx}$	=	Tosional, vertical and rotational frequency ratio values, respectively
ω	=	Excitation circular frequency
ω_n	=	Natural frequency of torsionally coupled system
$\omega, \omega_{\theta z}, \omega_v, \omega_{\theta x c}$	=	Translational, torsional, vertical and rotational natural frequencies, respectively
Ω_n	=	Coupled natural frequency ratio (ω_n/ω_u)
ρ_a, ρ_b	=	Mass densities of two halves of equivalent floor disc

REFERENCES

Decaninni, L.D., L. Liberatore and F. Mollaiolli, 2002. Response of bare and infilled R.C. frames under the effect of horizontal and vertical seismic excitation. Proceedings of the 12th European Conference on Earthquake Engineering, September 9-13, Elsevier Science Ltd., London, pp: 164-164.

Diotallevi, P.P. and L. Landi, 2000. Effect of axial force and of the vertical ground motion component on the seismic response of R/C frames. Proceedings of the 12th World Conference on Earthquake Engineering, New Zealand, 30 January-4 February, New Zealand Society for Earthquake Engineering, pp: 1026-1026.

Diotallevi, P.P. and L. Landi, 2006. Response of structures subjected to horizontal and vertical ground motions. Proceedings of the 8th US National Conference on Earthquake Engineering, August 18-22, Earthquake Engineering Research Institute, MIRA Digital Publishing, CD-ROM, California, pp: 1955-1955.

Foutch, D.A., 1997. A note on the occurrence and effects of vertical earthquake ground motion. NCEER-97-0010. Proceedings of the FHWA/NCEER Workshop on the National Representation of Seismic Ground motion for New and Existing Highway Facilities, Buffalo, September 1997, NCEER (National Center for Earthquake Engineering Research), pp: 253-257.

Ghobarah, A. and A.S. Elnashai, 1998. Contribution of vertical ground motion to the damage of R/C buildings. Proceedings of the 11th European Conference on Earthquake Engineering, September 6-11, Balkema, Rotterdom, Paris, pp: 468-468.

Gupta, R.K. and G.L. Hutchinson, 1994. Horizontal and vertical seismic response of torsionally coupled buildings. J. Eng. Struct., 16: 11-24.

Hosseini, M. and M.F. Nezamabadi, 2004. A study on the effect of vertical ground acceleration on the seismic response of steel buildings. Proceedings of the 13th world Conference on Earthquake Engineering, Vancouver, August 1-6, MIRA Digital Publishing, Canada, pp: 2377-2377.

Kianoush, M.R. and J.Z. Chen, 2006. Effect of vertical acceleration on response of concrete rectangular liquid storage tanks. J. Eng. Struct., 28: 704-715.

Kikuchi, K. and K. Yoshimura, 1984. Effect of vertical component of ground motions and axial deformation of columns on seismic behavior of RC building structures. Proceedings of the 8th world Conference on Earthquake Engineering, California, July 21-28, Earthquake Engineering Research Institute (EERI), pp: 599-606.

Memari, A.M., H. Maneetes and Y. Bozorgnia, 2004. Study of the effect of near-source vertical ground motion on seismic design of precast concrete cladding panels. J. Architectural Eng., 10: 167-184.

Papazoglou, A.J. and A.S. Elnashai, 1996. Analytical and field evidence of the damaging effect of vertical earthquake ground motion. J. Earthquake Eng. Struct. Dyn., 25: 1109-1137.

Rutenberg, A., 1998. EAEE TASK group (TG) 8: Behaviour of irregular and complex structures-state of the art report: Seismic nonlinear response of code-designed asymmetric structures. Proceedings of the 11th European Conference on Earthquake Engineering, September 6-11, Balkema, Rotterdom, Paris, pp: 651-651.

Stefano, M.D. and B. Pintucchi, 2002. A model for analyzing inelastic seismic response of plan-irregular building structures. Proceedings of the 15th ASCE Engineering Mechanics Conference, June 2-5, Columbia University, New York, pp: 494-494.

Wang, Z., D. Huo and X. Li, 1989. Analysis of seismic response for high-rise building structure under vertical ground motion. Proceedings of the 9th world Conference on Earthquake Engineering, Tokyo, August 3-9, WCEE Organization Commite, Japan, pp: 471-475.

Xinle, L., D. Huijuan and Z. Xi, 2007. Engineering characteristics of near-fault vertical ground motions and their effect on the seismic response of bridges. J. Earthquake Eng. Eng. Vibration, 6: 345-350.